

# A Turbine-Based Combined Cycle Solution for Responsive Space Access

Eklund, D. R.\* and Boudreau, A. H.†

*Aerospace Propulsion Division, Air Force Research Laboratory, Wright-Patterson AFB, OH 45433*

Bradford, J.E.‡

*SpaceWorks Engineering, Inc. (SEI), Atlanta, GA*

Reducing the time required to deliver payloads to low earth orbit is an objective of the U.S. military today given the growing dependence on space assets. This work presents one solution to this requirement. It is based on a fully reusable first stage space operations vehicle, called *Quicksat*, capable of satisfying multiple missions including the delivery of orbital payloads. *Quicksat* employs advanced turbojet engines and dual-mode scramjet engines and is hydrocarbon-fueled to enhance launch flexibility and responsiveness. The use of air-breathing propulsion systems also provides loiter capability, flyout and abort options. *Quicksat* appears to be a viable solution for providing responsive space access to the U.S. Air Force. The objective of this work is to outline the preliminary design of *Quicksat*, to provide details of several features of the design and to examine the sensitivity of the design to the propellant selection.

## Nomenclature

ACC	=	advance carbon-carbon
ACS	=	attitude control system
AFRL	=	Air Force Research Laboratory
AFRSI	=	advanced, flexible reusable surface insulation
APAS	=	aerodynamic preliminary analysis system
Aref	=	reference area (ft <sup>2</sup> )
CRI	=	conformal reusable insulation
C/Sic	=	carbon/silicon-carbide
Ct	=	thrust coefficient (thrust/q/Aref)
DMSJ	=	dual-mode scramjet
GTOW	=	gross take-off weight (lbs)
H <sub>2</sub> O <sub>2</sub>	=	hydrogen-peroxide
Isp	=	specific impulse (seconds)
JP-7	=	hydrocarbon jet fuel
LEO	=	low earth orbit
MPS	=	main propulsion system
MSP	=	military space plane
NASCART-GT	=	numerical aerodynamic simulation via cartesian grid techniques
RMS	=	root mean squared
S/HAPB	=	supersonic/hypersonic arbitrary body program
SMV	=	space maneuvering vehicle
SOV	=	space operations vehicle
T	=	temperature (R)
T <sub>s</sub>	=	surface temperature (R)
TPS	=	thermal protection system

\* Aerospace Engineer, Propulsion Technology Branch, AFRL-WPAFB and Senior Member AIAA.

† Chief, Propulsion Technology Branch, AFRL-WPAFB and Associate Fellow AIAA.

‡ President, SEI and Member AIAA.

<i>TSTO</i>	=	<i>two-stage to orbit</i>
<i>TUFI</i>	=	<i>toughened unifibrous flexible insulation</i>
<i>UHTC</i>	=	<i>ultra high temperature ceramic</i>
<i>k</i>	=	<i>thermal conductivity (btu/s/ft/R)</i>
<i>pcf</i>	=	<i>pounds per cubic foot</i>
<i>psf</i>	=	<i>pounds per square foot</i>
<i>q</i>	=	<i>dynamic pressure (lbs/ft<sup>2</sup>)</i>
<i>q<sub>conv</sub></i>	=	<i>convective heat transfer</i>
<i>s</i>	=	<i>seconds</i>
<i>t</i>	=	<i>time (seconds)</i>
<i>x</i>	=	<i>distance (ft)</i>
<i>α</i>	=	<i>angle-of-attack (degrees)</i>
<i>ε</i>	=	<i>emissivity</i>
<i>γ</i>	=	<i>thermal diffusivity (ft<sup>2</sup>/s)</i>
<i>σ</i>	=	<i>Stefan-Boltzmann constant</i>

## I. Introduction

The United States and the U.S. military in particular are increasingly dependent on space resources (i.e. satellite imagery, telecommunications, etc.). To respond with agility in space, a military space plane (MSP) has been proposed<sup>1,2</sup>. The core component of the MSP is the Space Operations Vehicle (SOV), which is a reusable first stage capable of servicing multi-role missions including delivering payloads to low earth orbit (LEO) with a turnaround time of hours rather than months.

Concurrently, in 2000-2001, the Air Force Research Laboratory (AFRL) and the Air Force Space Command (AFSPC), along with the Space and Missile Systems Center (SMC), embarked on a technology planning process entitled “Technology Planning Integrated Product Team” or TPIPT. The Launch Operations facet of this effort invited concepts for improved space-lift to be submitted by both industrial and government organizations. The vast majority of these concepts dealt with rocket-propelled systems. Only AFRL’s Propulsion Directorate provided an air-breathing hypersonic concept. That concept was called “Quicksat” in light of the system’s ability to execute launch operations in a fast-response, wartime environment. At the time of that submission, only an in-house conceptual analysis of the system had taken place. A more rigorous analysis and conceptual design was required to substantiate claims of system performance.

In 2003 the Aerospace Propulsion Division of AFRL’s Propulsion Directorate contracted with SpaceWorks Engineering Inc. to provide the conceptual *Quicksat* design. The *Quicksat* vehicle operates as the first stage of a Two-Stage-To-Orbit (TSTO) launch system. A variety of second-stage vehicles could be carried on the first-stage *Quicksat*. The *Quicksat* concept uses a combined-cycle approach where high-speed turbojet engines are combined with a hydrocarbon-fueled dual-mode scramjet and hydrocarbon-fueled rockets to produce a cost-effective system with aircraft-like operations. This paper summarizes that design effort and highlights features of the design. In addition, the impact of the fuel and oxidizer propellant choice is investigated.

## II. *Quicksat* Vehicle Overview

The *Quicksat* SOV is the first element of a two-stage MSP concept that uses combined-cycle air-breathing propulsion (see Fig. 1). The nominal system takes off and lands horizontally and uses non-cryogenic propellants for improved operability in support of on-demand and responsive launch scenarios. The booster is capable of supporting three different missions: a) space maneuvering vehicle (SMV) delivery to orbit, b) a hypersonic strike mission, and c) cargo delivery to LEO and polar orbits by configuring the upperstage with mission-specific hardware.

The nominal mission for the *Quicksat* is the delivery of an SMV to an elliptic 70x197 nmi. orbit at a 28.5° inclination and is the focus of this study. The SMV is a reusable vehicle capable of remaining on-orbit for extended periods of time<sup>3,4</sup>. The vehicle features a small, kerosene/H<sub>2</sub>O<sub>2</sub> liquid rocket engine (Rocketdyne AR2-3) for on-orbit maneuvering. The total vehicle weight is 13,090 lbs, which includes an experiment bay with up to 500 lbs. of payload. The length from nose-to-tail is 27.5 ft and the wingspan is 15.0 ft.



**Figure 1. *Quicksat* Launch from Notional Military Facility.**

The SMV is deployed by an expendable rocket-powered upperstage. This stage consists of 3 propellant tanks, an attitude control system (ACS), flight controller, thermal protection system (TPS) blankets, and a single liquid rocket engine. The SMV is attached at its base to the forward section of a truss structure. The upperstage engine accelerates the SMV from Mach 8 to orbital velocities using JP-7 and H<sub>2</sub>O<sub>2</sub> propellants. Figure 2 shows an external view of the SMV and the SMV attached to the expendable upperstage system.

The expendable upperstage hardware elements are designed with limited reliance on new technology developments to keep the recurring system costs to a minimum. The engine is a derivative of the reusable engines on the *Quicksat* booster (described below) and the propellant tanks are all constructed from aluminum. The ACS is a simple blow-down, pressure-fed, monopropellant arrangement using H<sub>2</sub>O<sub>2</sub>. The upper half of the body is covered in thermal blankets to protect the hardware during the ascent, prior to booster release. Since the system is unmanned, minimal system redundancy has been used. The integrated system has a combined weight of 90,215 lbs. and the total stage length is 52.2 ft including the SMV.

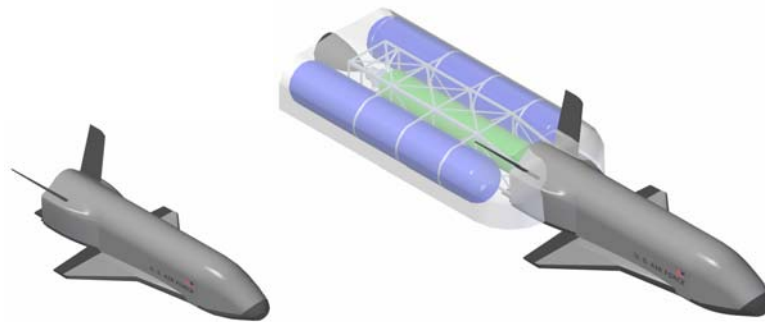


**Figure 2. SMV and SMV+Upperstage System**

The *Quicksat* booster is configured as a lifting-body design, derived from the National Aerospace Plane (NASP) program vehicle configurations and similar to the NASA Hyper-X (X-43) integrated-scrumjet flight test program<sup>5</sup>. Upperstage modules are located on the leeward, aft portion of the vehicle in a partially recessed cavity. The air-breathing propulsion systems are arranged in an over-under configuration with turbine-engines embedded in the vehicle airframe and an underslung dual-mode scumjet (DMSJ) system. These engines share a common external compression system (i.e. the vehicle forebody) and aftbody expansion zones. In addition to providing engine airflow matching and optimal flow expansion, the variable geometry inlet and exit ramps can shield the turbine systems

from the freestream flow when not being operated. All propulsion system elements use JP-7 hydrocarbon fuel. The rocket systems also use a hydrogen-peroxide ( $H_2O_2$  at a 95% purity level) oxidizer.

*Quicksat* takes off under the power of six advanced, low-bypass ratio turbofan engines fueled with JP-7. The engines operate up to Mach 3.75 and are grouped in pairs with each pair sharing a common inlet and nozzle ramp. At sea-level static conditions, each engine provides 65,660 lbs of thrust using its afterburner with a corresponding ISP of 1895 s. The engines have an installed T/W of 10.0.

Four dual-mode scramjet DMSJ engines operate from Mach 3.75 to Mach 8. The engines also use JP-7 fuel and are assumed to be regeneratively cooled. Other features of the DMSJ engines include a three-ramp two-dimensional external compression system, variable geometry inlets and a thermal choke in the nozzle section. At a vehicle angle of attack of  $0^\circ$  and a dynamic pressure of 2000 psf, the engine ISP equals 1678, 975 and 771 s at a flight Mach number of 4, 6 and 8, respectively. The corresponding coefficient of thrust,  $C_t$ , is 0.82, 0.59 and 0.43, respectively. The reference area for  $C_t$  equals 320.8  $ft^2$ .

*Quicksat* also houses four tail-rockets that provide thrust during the transonic flight regime and during the pullup maneuver before staging. The tail-rockets use JP-7 and  $H_2O_2$  propellants, both non-cryogenic fluids for ease in handling and extended ground-hold times. The engines are a closed-cycle design with parallel flow turbine gases that are generated from a hydrogen-peroxide catalyst pack. The configuration reduces pump weight by eliminating the need to boost the fuel to excessively high pressures normally required for a bipropellant preburner design. Several key performance parameters are provided in a later section.

The feasibility and viability of the *Quicksat* system is dependent upon technology advances in a number of key areas. Specific technologies employed by the booster system include: graphite-epoxy (Gr-Ep) airframe primary and secondary structures, titanium-aluminide wing and tail hot structures, cylindrical, non-integral Gr-Ep fuel tanks and aluminum oxidizer tanks, electro-hydraulic actuators (EHAs) for control surfaces, and all-moving vertical tails.

The internal airframe components were arranged to provide the best overall packaging efficiency while not compromising the ability to access and inspect the vehicle's propellant tanks, feed lines, propulsion systems, and subsystems. Additionally, denser items such as oxidizer tanks and subsystems were located as far forward as possible to prevent the vehicle center-of-gravity (C.G.) from being located too far aft. Figure 3 provides various transparent views of the airframe and internal systems.

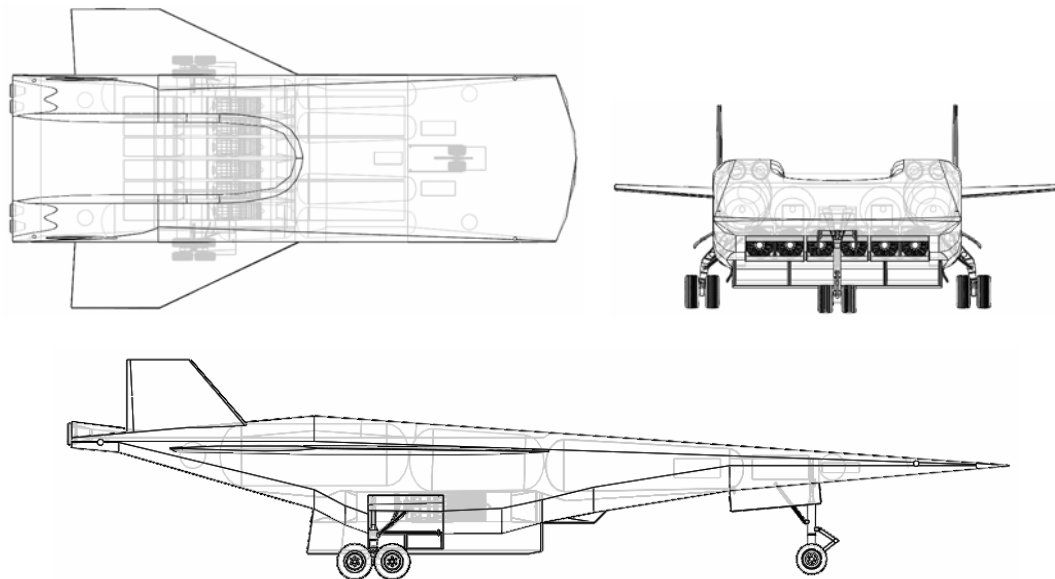


**Figure 3. *Quicksat* Internal Views.**

The length of the *Quicksat*, from the nose-to-tail section is 123.6 feet, with a wingspan of 65 feet and tail height of 26 feet. The weight of the booster, without propulsive fluids, is 167,840 lbs. Without an upperstage module, the weight of the fully loaded booster with the JP-7 fuel and  $H_2O_2$  oxidizer propellants is 651,455 lbs, yielding a total gross takeoff weight (GTOW) of 741,670 lbs. (less startup losses) for the SMV deployment mission. Further details of the *Quicksat* space-lift system are provided in Ref. 6.

### III. Overview of Conceptual Design Methodology

The complex vehicle architecture was designed and analyzed using a collaborative, distributed framework known as ModelCenter<sup>®</sup> available from Phoenix Integration, Inc.<sup>7</sup>. A number of industry standard analysis tools were utilized, along with numerous in-house codes developed at SEI.

Industry codes included:

- POST 3-degree of freedom trajectory simulation code<sup>8</sup>
- APAS - S/HABP aerodynamic and aeroheating load predictions<sup>9</sup>
- NASCART-GT 3-D Euler with external flowfield analysis<sup>10</sup>
- NEPP turbine system performance tool<sup>11</sup>
- SRGULL scramjet engine performance analysis
- Solid Edge configuration layout and center-of-gravity assessments

Codes developed by SEI include:

- REDTOP attitude control system (ACS) performance predictions<sup>12</sup>
- REDTOP-2 liquid rocket engine design<sup>13</sup>
- SEI-Sizer airframe, tank, and subsystem weight modeling and system sizing
- SENTRY transient, 1-D aeroheating analysis and thermal protection system design/sizing
- SESAW avionics subsystems

The disciplinary tools with tightly coupled variables (between multiple disciplines) were integrated together to create an automated system closure model. Non-dimensional parameters like the aerodynamic coefficients and air-breathing propulsion system thrust coefficient permit scaling within reasonable ranges through normalization with a reference area. Figure 4 illustrates the coupling between disciplines in the performance closure process. Details of the aerodynamics, trajectory and aeroheating/TPS modules will be presented later in this work.

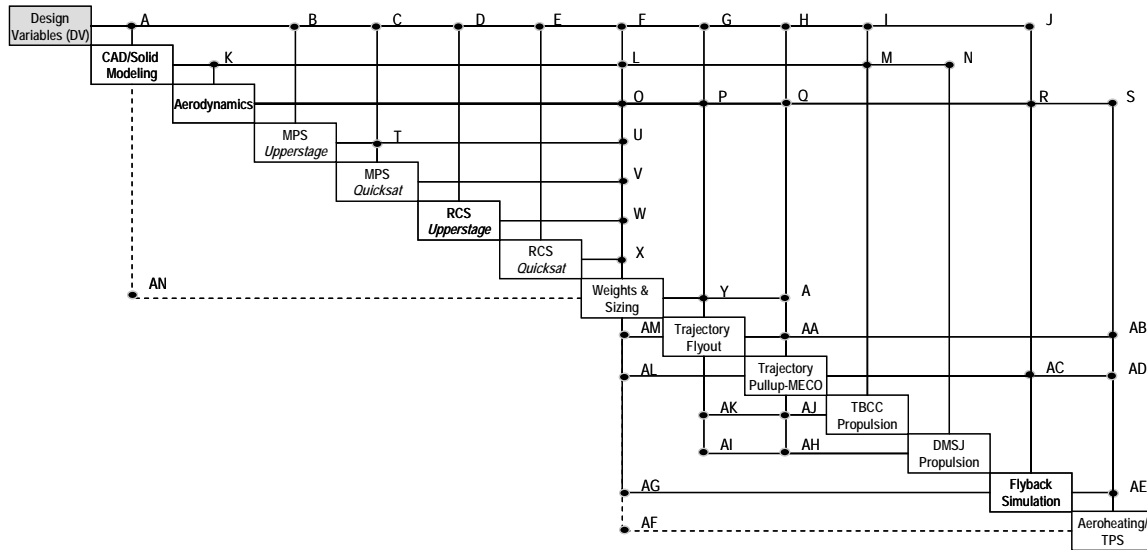


**Figure 4. Design Structure Matrix (DSM) Employed During the Performance Closure Process (Dotted Lines Indicate Weak Coupling).**

## IV. Features of the Conceptual Design

### A. Mission Profile

The system nominally launches from Cape Canaveral at approximately  $28.5^\circ$  latitude. Figure 5 displays the Mach number history for both stages, in addition to the angle of attack and dynamic pressure histories for the *Quicksat* booster. The vehicle takes off under power provided from its six advanced turbine engines. A rotation maneuver is executed that pitches the *Quicksat* up from  $\alpha=0^\circ$  to  $\alpha=20^\circ$ , enabling a takeoff speed of 291 kts and requiring approximately 10,560 ft. of runway length. The *Quicksat* accelerates and climbs to Mach 0.8 ( $t=220$ s) at which point the flight system ignites the four JP-7/LOX tail- rockets. These rockets operate through transonic up to Mach 1.4 ( $t=270$  s), where turbine-only power can be resumed. The *Quicksat* continues to accelerate reaching a dynamic pressure of 1,600 psf at Mach 3.75 ( $t=1145$  s).

The vehicle subsequently transitions from turbine to DMSJ power by executing a rapid series of shut-down and

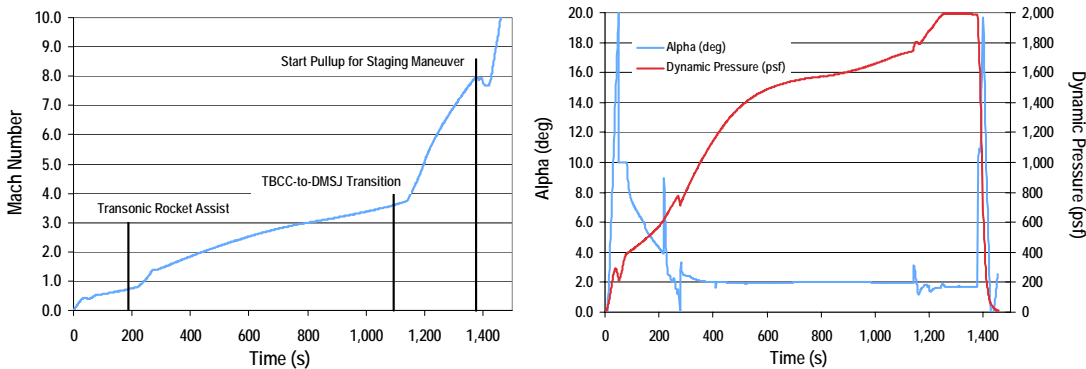


**Figure 5. Mach Number History for TSTO System and Angle of Attack and Dynamic Pressure Histories for *Quicksat*.**

power-up procedures, respectively. The inlet ramps to the turbine engines are retracted to cut off the air inflow, fuel flow is gradually reduced to permit additional cooling, and the nozzle ramps are finally closed. Simultaneously, the JP-7 fuel flowrate to the DMSJ engines is rapidly increased. In the trajectory simulation two seconds of unpowered flight separates turbojet and DMSJ operation. The DMSJ engines operate in a fuel-lean mode until the flight speed increases enough to maintain the thermal choke at the nominal fuel-rich ( $\phi=1.1$ ) conditions. The vehicle operates under DMSJ power and along a dynamic pressure boundary of 2,000 psf up to Mach 8 ( $t = 1375$  s).

Upon reaching Mach 8, the vehicle departs from the  $q$ -boundary and begins a sharp pull-up maneuver to setup the staging event. Within a few seconds the dynamic pressure drops below 500 psf and the controller signals the tail-rocket re-ignition. The tail-rocket and DMSJ engines are burned simultaneously during the pullup maneuver. The Mach number at the rocket re-ignition is still approximately 8 due to atmospheric impacts on the speed of sound. The tail-rockets are then used to boost the vehicle to the Mach 9 staging condition at an altitude of 250,000 ft ( $q=25$  psf).

At the staging point, the attach clamps for the upperstage are released and the single tail-rocket is ignited. Under all-rocket propulsion, the upperstage continues to the insertion velocity at an altitude of 70 nmi. After staging, the *Quicksat* continues to reduce its speed and performs an unpowered turn towards the launch site. When the vehicle has reduced its speed and altitude to Mach 5 at an altitude of 95,000 ft ( $q\sim 500$  psf), the DMSJ engines are restarted and used to fly the vehicle back to the launch site. The total flyback distance of approximately 775 nmi. requires 0.26 hours to complete.

As seen in Fig. 5, the total ascent time-to-orbit for the SMV is 0.47 hours from launch, with the staging maneuver occurring at 0.40 hours into the mission. In the event that *Quicksat* can return to a downrange base for service and propellant resupply, a partial amount of the flyback propellants can be used to either loiter or to change the launch azimuth and obtain the desired orbital plane.

The transition from turbojet to DMSJ operation is also observed in Fig. 5 and occurs 0.32 hours from launch. Hence, obtaining Mach 3.75 represents approximately 2/3 of the total ascent time-to-orbit. Figure 6 illustrates the

cause of the sluggish acceleration under turbojet power. The net ISP equals the engine thrust divided by the propellant flow rate, while the effective ISP accounts for the vehicle drag. At Mach 3.75,  $Q \approx 1750$  psf, the DMSJ engines have a higher net ISP than the turbojet engines. More significantly, the four DMSJ engines at this condition produce approximately twice the thrust of the six turbojet engines. Consequently, the vehicle's effective ISP is improved due to the higher thrust output of the DMSJ systems and thus greater thrust minus drag margin. Increasing the *Quicksat* acceleration during turbojet operation could be obtained by increasing the size and/or the number of turbine engines (the takeoff T/W equals 0.53). However, that may entail adding a second row of turbine engines, which would increase inlet and nozzle complexity and overall vehicle complexity considerably. Alternatively, the tail-rockets can be operated beyond Mach 1.4. Throttling the tail-rockets to 50% power from Mach 1.4 to the DMSJ transition (Mach 3.75) reduced the time to reach Mach 8 from 1375 s to 700 s and reduced the flyback distance from 775 nmi. to 440 nmi. The GTOW and *Quicksat* dry weight also decreased by 6% and 8%, respectively.

The SMV obtains a net velocity of 24,540 ft/s at orbit, while the gross velocity change for the nominal trajectory is 45,095 ft/s. The loss components are drag, gravity, atmosphere (i.e. backpressure losses during rocket operation) and thrust vector control (i.e. nonalignment of the thrust vector with the flight angle due to the angle of attack). Figure 7 displays the various components of the aggregate change in velocity.

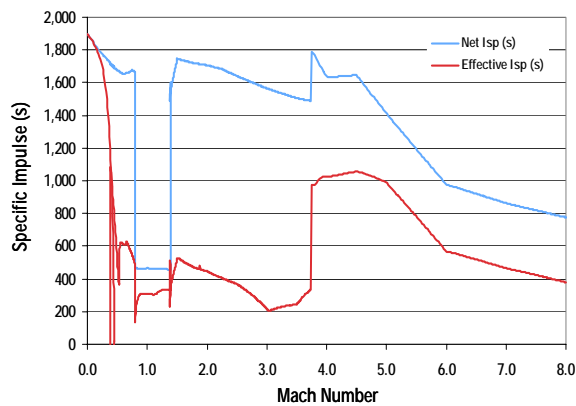


Figure 6. Net and Effective ISP for the *Quicksat* Booster.

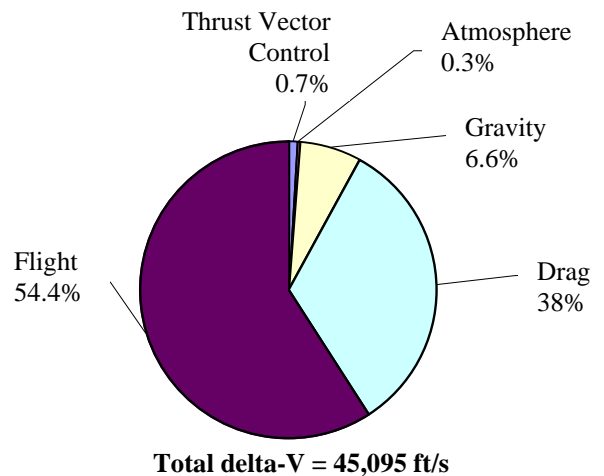


Figure 7. Breakdown of Delta-V Components.

## B. Aerodynamics

Aerodynamic data for *Quicksat* was obtained from the Aerodynamic Preliminary Analysis System (APAS) developed by NASA and Rockwell International and used in designing the Space Shuttle. The APAS program contains two programs: a vortex panel code called Unified Distributed Panel for subsonic and low supersonic flow conditions and the Supersonic/Hypersonic Arbitrary Body Program (S/HABP) for hypersonic flow conditions that uses a local surface inclination method. The geometry used for the analysis is shown in Fig. 8 and contained approximately 2000 surface nodes. The calculated lift and drag coefficients are shown in Fig. 9 for the nominal trajectory. The spikes result from 1) a rotation maneuver at takeoff that increases  $\alpha$  from  $0^\circ$  to approximately  $20^\circ$ , 2) rapid changes in the angle of attack associated with thrust deltas during ignition and shut-down of the tail rockets and 3) the turbojet to DMSJ transition point. There is not an

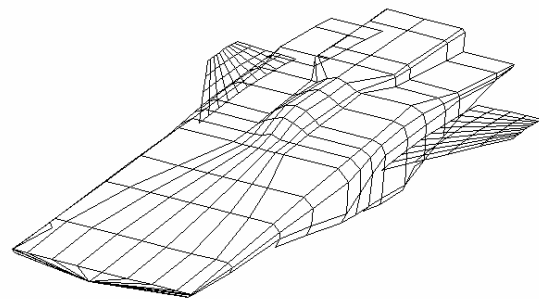
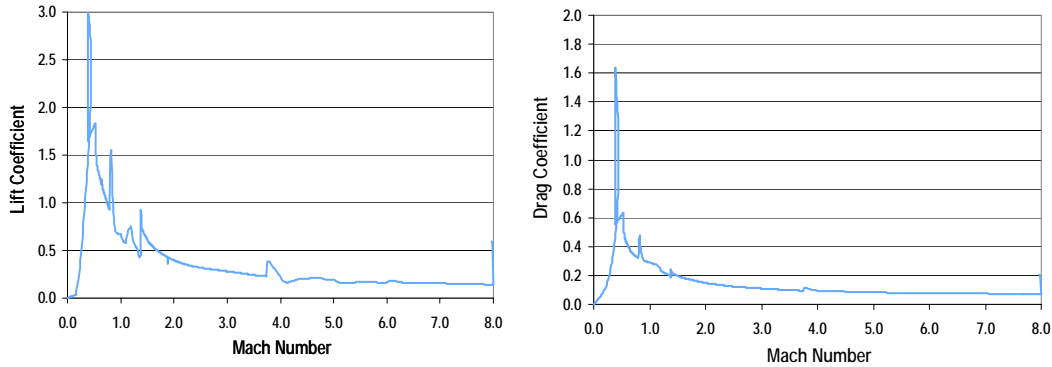


Figure 8. Geometry used for APAS analysis.

appreciable drag rise near  $M=1$ , because the POST optimizer forces *Quicksat* to a lower angle of attack when pushing through transonic to mitigate the drag rise (see Fig. 5). Representative values for  $L/D$  are 2.68, 2.41, 2.07 and 1.97 for Mach = 2, 4, 6 and 8, respectively.



**Figure 9. Lift and Drag Coefficients vs. Flight Mach Number**

To verify the fidelity of the aerodynamic data from APAS, CFD solutions were obtained at several conditions using the Numerical Aerodynamic Simulation via CARTesian Grid Techniques (NASCART-GT) program. The program employs automated grid generation that adapts to the solution using either the divergence of velocity or the vorticity as the adaptation criteria. NASCART-GT solves the Euler equations, the Euler equations coupled with an integral boundary layer solution technique or the Navier-Stokes equations. In this study simulations were performed at  $\alpha=5^\circ$  for  $M=0.4, 1.05, 3.0, 5.0$  and  $8.0$  and at  $\alpha=0^\circ$  and  $10^\circ$  for  $M=3.0, 5.0$  and  $8.0$  employing the Euler equations with an appropriate integral boundary layer method. The simulations did not include the propulsive flow fields. The divergence of velocity was selected as the grid adaptation criteria and the convergence criteria was either a maximum RMS residual of  $1 \times 10^{-5}$  or 10000 iterations.

Solutions obtained at  $\alpha=5^\circ$  for  $M=1.05$  and  $5.0$  are displayed in Fig.'s 10 and 11. Approximately, eight grid adaptations were performed and the calculation was stopped after 10000 iterations for both solutions. Figure 10 shows contours of the normalized pressure and the computational mesh along the centerline plane for the  $M=1.05$  case. A weak bow shock is generated upstream of the vehicle. The shock decelerates the flow to subsonic conditions on both the upper and lower surfaces. Along the lower surface, localized high pressure regions are observed from the three-ramp external compression system. Rapid acceleration of the flow is observed near the rear of the vehicle on both the upper and lower surfaces before traversing shocks that act to match the upper and lower vehicle pressures as the flows come together at the trailing edge. The final computational grid has successfully adapted to the features of the flow field as seen in Fig. 10.

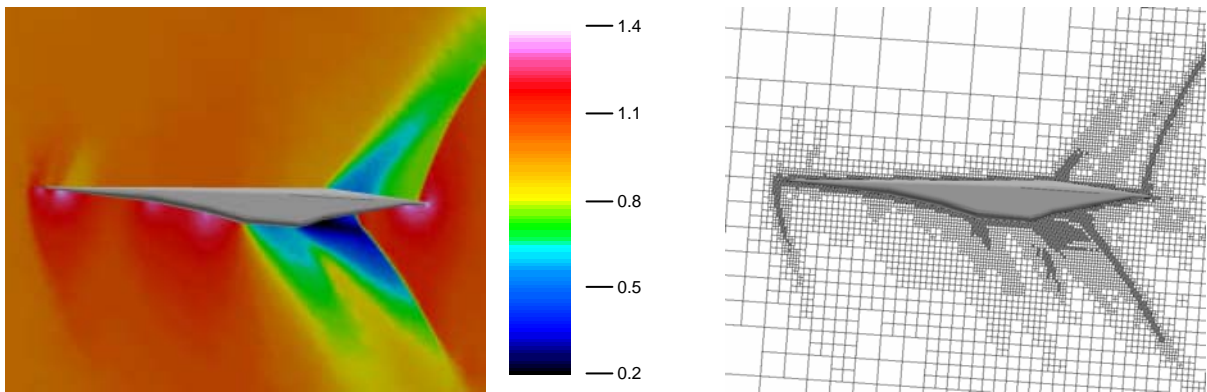


**Figure 10. Normalized Pressure Contours and Computational Mesh for  $M=1.05$  and  $\alpha=5^\circ$ .**

Normalized pressure contours along the centerline plane from the  $\alpha=5^\circ$ ,  $M=5.0$  case is shown in Fig. 11. The flow appears uniform along the fore upper surface, because it is inclined at four degrees, hence for  $\alpha=5^\circ$  the flow experiences only a  $1^\circ$  expansion. Along the lower surface oblique shocks from the three ramp compression system decelerate the flow. Expansion surfaces at the rear of vehicle along the top and lower surfaces reduce the pressure and accelerate the flow. A three-dimensional view is given in Fig. 12 which shows pressure contours along the surface of the vehicle and Mach number contours enveloping the vehicle. The high pressure flow generated by the three-ramp compression system is effectively contained within the lower surface.

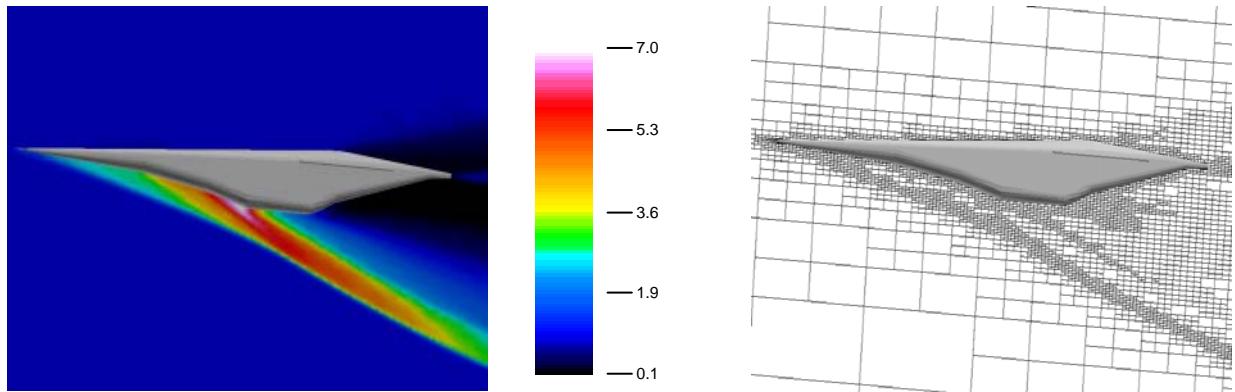


**Figure 11. Normalized Pressure Contours and Computational Mesh for  $M=5.0$  and  $\alpha=5^\circ$ .**

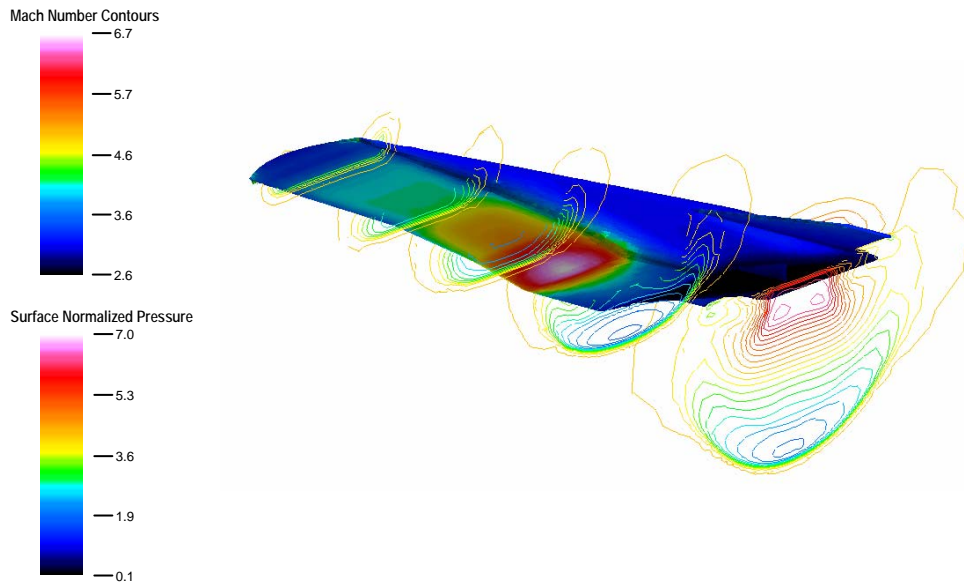


**Figure 12. Flow Field Mach Contours and Surface Normalized Pressure Contours for  $M=5.0$  and  $\alpha=5^\circ$ .**

Comparisons of the integrated Cd values are shown in Fig. 13 for M=3.0, 5.0 and 8.0 at  $\alpha=0^\circ$ ,  $5^\circ$  and  $10^\circ$ . Agreement degrades as  $\alpha$  increases, but appears quite reasonable over the range that *Quicksat* accesses during its flight, which is  $0^\circ \leq \alpha \leq 4^\circ$ .

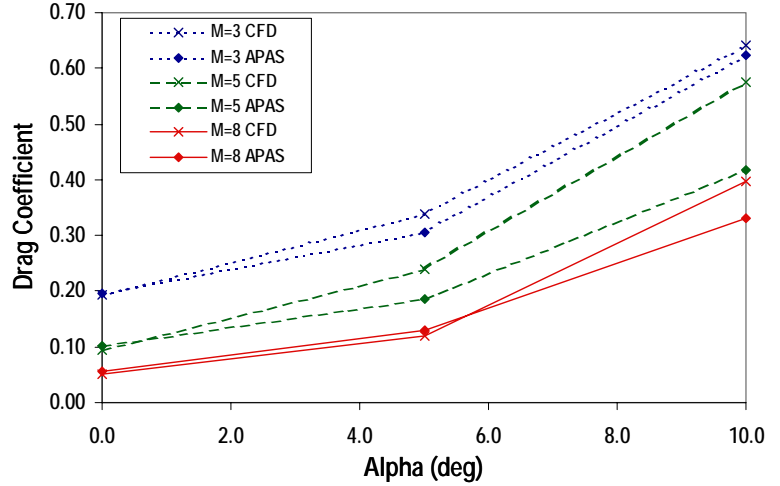


**Figure 13. Comparison of APAS and NASCART-GT Drag Coefficients versus Angle of Attack.**

### C. Aeroheating and Thermal Protection System

All of the thermal protection systems (TPS) used by the booster and orbiter are passive due to the relatively low hypersonic Mach number envelope. The TPS for *Quicksat* was designed with SENTRY developed by SpaceWorks Engineering, Inc. SENTRY solves the 1D unsteady heat equation for each TPS panel:

$$\frac{\partial T}{\partial t} = \gamma \frac{\partial^2 T}{\partial x^2} \quad (1)$$

The boundary condition on the top surface accounts for conduction, convection and radiation:

$$q_{conv} - \epsilon \sigma T_s^4 + k \frac{dT}{dx} = 0 \quad (2)$$

and the backface surface is assumed to be adiabatic ( $dT/dx = 0$ ) which yields a conservative design. The S/HABP code provided the heating rate ( $q_{conv}$ ) as a function of time using the trajectory data obtained from POST (e.g. Mach, altitude and  $\alpha$  vs. time) and the surface temperature equaled the radiation equilibrium temperature.

SENTRY includes over 80 different TPS and structural materials (e.g. metals, composites and blankets). Each candidate stackup arrangement includes several material and TPS types. For instance, TUFU AETB-8 ceramic tiles contain six material layers: 1) TUFU (Toughened Unifibrous Flexible Insulation) coating (0.1 in. thickness), 2) AETB diffusion layer (0.1 in. thickness), 3) AETB-8 which is an 8 pcf fibrous insulation substrate (variable thickness), 4) room temperature vulcanizing (RTV-560) silicone adhesive (0.0075 in. thickness), 5) Strain Isolation Pads (SIPs) (0.0075 in. thickness) and 6) room temperature vulcanizing (RTV-560) silicone adhesive (0.0075 in. thickness). The SIPs and RTV-560 adhesive are used to attach each tile to the airframe. Approximately five stackup arrangements were considered for each surface element. Other stackup arrangements considered included Conformal Reusable Insulation (CRI), a silica-based batting called Advanced Flexible Reusable Surface Insulation (AFRSI) blankets, advanced carbon-carbon (ACC) sheets, Carbon/Silicon-Carbide (C/SiC) sheets and hafnium-diboride (HfB2) Ultra High Temperature Ceramic (UHTC).

Each stackup material was assessed by SENTRY on a vehicle analysis grid that consisted of 2,048 nodes. The grid was similar to the grid used for the APAS analysis (Fig. 8), but included the vehicle tails and possessed a smooth upper surface. The aeroheating analysis started at Mach = 1.25, with a uniform structure temperature of 600 R. The analysis modeled the flyout, pullup, staging maneuver, flyback and a two-hour cool down/thermal soak period. A constant emissivity of 0.8 was used for all surfaces and the vehicle was assumed to have a leading edge radius of two inches. The backface temperature for the airframe was required to not exceed 760 R, while the backface temperature for the wings and tails was limited to 950 R. Also, the maximum material temperature for the AFRSI blankets, TUFU tiles and ACC are 1660 R, 2860 R and 3360 R, respectively. The CRI, C/SiC and UHTC materials have a maximum temperature of 2000 R, 3460 R and 4460 R, respectively. The optimal TPS type is determined at each node by considering the thickness manufacturing constraints, maximum reuse surface

temperatures, and the minimum weight. The resulting materials and their weights selected by the analysis are listed in Table 1. The average unit weight for all the TPS materials is 1.348 lbs/ft<sup>2</sup>.

The majority of the windward surfaces of the airframe are covered with CRI, although the nozzle employs TUF1 ceramic tiles. The leeward surfaces of the airframe are covered with AFRSI blankets. The vehicle has sharp leading edge radius of 2 inches which results in stagnation point temperatures exceeding 3,000 R and requires the use of ACC. The bulk area of the upper and lower wing and tail surfaces are covered with CRI, while the control surfaces and leading edges are covered with ACC.

**Table 1. TPS Materials Employed by Quicksat**

Component – Fuselage	Material Stackup	Avg. Unit Weight
Leeward and Sidewalls	AFRSI Blankets and CRI	0.75 psf
Windward Forebody and Aftbody Nozzle	TUF1 AETB-8 Ceramic Tiles and CRI	1.47 psf
Nose	ACC	12.6 psf
Component – Wings		
Leading Edges	ACC	12.6 psf
Windward Side	CRI	1.37 psf
Leeward Side	CRI	0.82 psf
Component – Tails		
Leading Edges	ACC	12.6 psf
Windward Side	CRI	0.82 psf
Leeward Side	CRI	0.82 psf

The maximum temperatures calculated for each vehicle panel is shown in Fig. 14. Away from the hot leading edges that are not visible in the figure, the peak surface temperature is approximately 2500 R. The aft portion of the windward surface of the airframe experiences higher temperatures, because the propulsive flow field is simulated by imposing the surface temperature. During the SENTRY calculation, the wing control surfaces are deflected upward 5° and downward 15° over the entire flight profile causing the increased temperatures seen in Fig. 14 for the control surfaces.

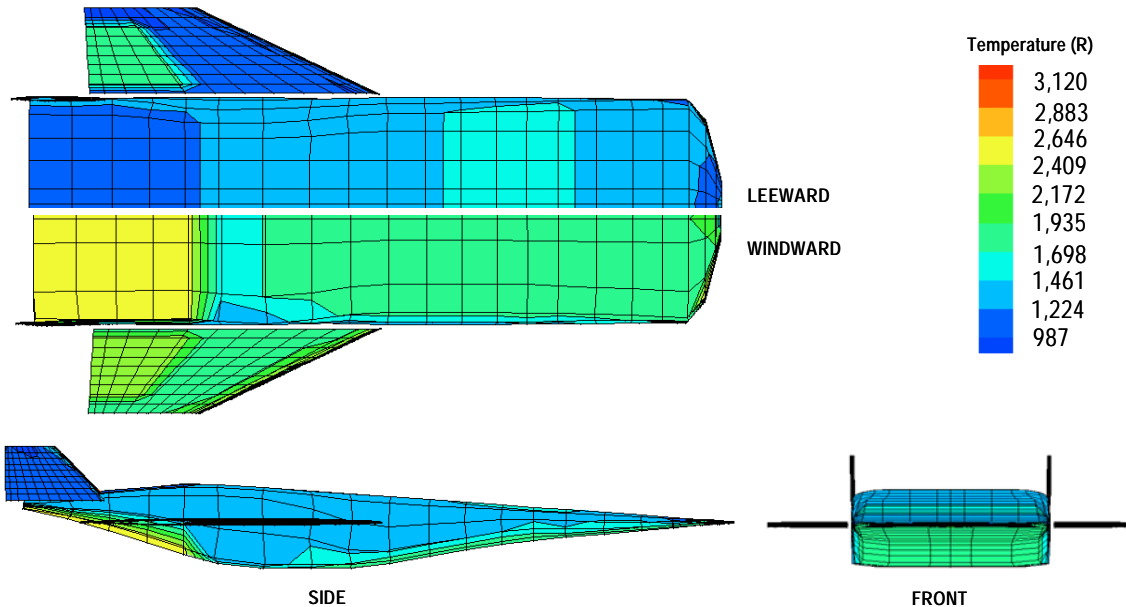


**Figure 14. Maximum temperature [R] encountered by *Quicksat* along the leeward, windward, side and front surfaces.**

## D. Propellant Selection

The nominal JP-7 and H<sub>2</sub>O<sub>2</sub> propellants for *Quicksat* are easily storable, non-cryogenics that were selected to enhance the responsiveness of the space-lift system. However, this class of propellants yields reduced rocket engine performance. Two alternate propellant combinations were evaluated to assess the impact of the propellant choice to the design. The first alternate combination replaces H<sub>2</sub>O<sub>2</sub> as the oxidizer with liquid oxygen (LOX). LOX provides a higher engine ISP at the expense of the tank insulation weight and lower density (71.2 vs. 89.5 pcf). Additionally, the main propulsion system (MPS) for the rocket is more complex. The JP-7/LOX rocket engine is a fuel-rich single-preburner staged combustion cycle engine with parallel flow turbines whereas the nominal MPS employed a closed-cycle design with a H<sub>2</sub>O<sub>2</sub> catalyst pack to generate the turbine drive gases. The second alternate propellant combination considered was C<sub>3</sub>H<sub>8</sub>/LOX. Soft-cryogen propane (C<sub>3</sub>H<sub>8</sub>) fuel also increases the engine specific impulse but at a lower density than JP-7 (36.0 vs. 50.3 pcf). Residues and coking within the fuel lines are reduced when replacing JP-7 with C<sub>3</sub>H<sub>8</sub>, which improves the maintainability and reusability of the engine. Methane has an even lower propensity for coking than propane, but the ignition delay for methane is significantly higher than for propane<sup>14,15</sup>. The lower reactivity of methane may compromise performance of the DMSJ engines. Consequently, a C<sub>3</sub>H<sub>8</sub>/LOX propellant combination was considered in this study.

Shown in Table 2 are selected propellant properties and system metrics for the three different propellant combinations examined at staging conditions of both Mach 9 and Mach 10. For both staging scenarios, the pullup maneuver commenced at Mach 8. The lower T/W for the two alternate propellant combinations that employ a staged combustion cycle is due to a higher fuel pump discharge pressure. Considering first the propellant selection impact for staging at Mach 9, the C<sub>3</sub>H<sub>8</sub>/LOX combination yields the lowest GTOW. Its GTOW represents an 18% reduction from the nominal system and is lower than the gross weight of a Boeing 777-300. The JP-7/LOX combination offers a compromise in propellant density and engine ISP and yields the minimum booster dry weight.

**Table 2. Propellant Study Results for Mach 9 and Mach 10 Staging**

Parameter	JP-7 and H <sub>2</sub> O <sub>2</sub> Propellants	JP-7 and LOX Propellants	C <sub>3</sub> H <sub>8</sub> and LOX Propellants
Propellant Density (lbm/ft <sup>3</sup> )	50.3 & 89.5	50.3 & 71.2	36.0 & 71.2
Booster Engine Vacuum T/W	90.1	81.1	79.9
Upperstage Engine Vacuum T/W	75.1	73.7	72.6
Booster Engine Vacuum Isp (s)	329.9	343.8	351.1
Upperstage Engine Vacuum Isp (s)	336.1	353.4	359.1
<b>Mach 9 Staging</b>			
System GTOW (lbs)	741,760	691,130	609,570
Booster Dry Weight (lbs)	167,840	164,030	168,650
Upperstage GTOW (lbs)	89,515	83,385	84,400
Upperstage Dry Weight (lbs)	4,275	4,410	4,780
Total Length (ft)	123.6	122.6	125.6
<b>Mach 10 Staging</b>			
System GTOW (lbs)	910,670	771,970	696,700
Booster Dry Weight (lbs)	199,110	181,220	189,960
Upperstage GTOW (lbs)	80,455	72,615	75,805
Upperstage Dry Weight (lbs)	3,915	3,935	4,360
Total Length (ft)	134.6	129.1	133.5

The system attributes for staging Mach number conditions of 9 and 10 are also provided in Table 2. The tail-rocket operation during the pullup maneuver is extended to support the higher staging condition at Mach 10. Staging at Mach 10 increases the GTOW by 22.7%, 11.7% and 14.3% for the JP-7/H<sub>2</sub>O<sub>2</sub>, JP-7/LOX and C<sub>3</sub>H<sub>8</sub>/LOX systems, respectively. The upperstage GTOW and empty weight is reduced by staging at Mach 10, though. The upperstage GTOW is reduced 10.1%, 12.9% and 10.2% and the upperstage empty weight is reduced 8.4%, 10.7% and 8.8%, respectively, for the JP-7/H<sub>2</sub>O<sub>2</sub>, JP-7/LOX and C<sub>3</sub>H<sub>8</sub>/LOX systems. Overall, the JP-7/LOX system is observed to be the least sensitive to the staging Mach number.

Selection of the propellants for a future SOV, such as *Quicksat*, must consider propellant handling and engine maintenance in addition to performance to enable a responsive, reusable space-lift system. The capabilities of the current industrial base for producing the propellants and the infrastructure for handling the propellants will also be factors in the selection.

## V. Conclusion

The preliminary design of a reusable Space Operations Vehicle powered by air-breathing propulsion systems, called *Quicksat*, is presented. *Quicksat* takes off and lands horizontally and is capable of supporting multiple missions including payload delivery to LEO. The gross takeoff weight for delivering a 13,090 lb space maneuvering vehicle to LEO is 741,670 lbs, which is lighter than a Boeing 747. The use of air-breathing propulsion and non-cryogenic fuels permits launch flexibility plus loiter capability, flyout and abort options. *Quicksat* provides a viable solution for achieving responsive space access.

Additionally, extending the use of the tail-rockets from transonic conditions to the transition to dual-mode scramjet operation was found to reduce the gross takeoff weight and the empty weight for *Quicksat*. The propellant options; JP-7/LOX and C<sub>3</sub>H<sub>8</sub>/LOX were also considered. The C<sub>3</sub>H<sub>8</sub>/LOX system yielded the lowest gross takeoff weight, while the JP-7/LOX system provided the lowest empty weight for *Quicksat*. Both JP-7/LOX and C<sub>3</sub>H<sub>8</sub>/LOX were found to reduce the sensitivity of the system to the staging Mach number. These performance gains must be weighed against the operational impact of using the soft-cryogenes.

Finally, the study of *Quicksat* reported here also encompassed an analysis of the non-recurring costs, vehicle safety and reliability, operations, and a Mission Effectiveness analysis. These metrics and system aspects will be presented in a future paper.

## Acknowledgments

The authors would like to recognize the contribution of Jon Wallace, Brad St. Germain and A.C. Charania from SpaceWorks Engineering, Inc. to the design of the *Quicksat* vehicle. The authors would like to thank Chris Snyder of NASA Glenn Research Center and Chuck Bauer of Universal Technology Corporation for their contributions to the low-speed engine system performance. The authors would also like to express their sincere appreciation to Glenn Liston from the Air Force Research Laboratory at Wright-Patterson Air Force Base for funding this work under Contract #F33615-03-C-2302.

## References

<sup>1</sup>NASA-USAF OneTeam, "The Military Space Plane: Providing Transformational and Responsive Global Precision Striking Power," Peterson AFB, Colorado, January 2002, on-line, Internet, 31 August 2004, available from: [http://www.wslfweb.org/docs/msp/military\\_spaceplane\\_utility.pdf](http://www.wslfweb.org/docs/msp/military_spaceplane_utility.pdf).

<sup>2</sup>Anttonen, John, Capt., "U.S. Air Force Space Operations Vehicle", AIAA98-1568, 8<sup>th</sup> International Space Planes and Hypersonic Systems and Technology Conference, Norfolk, VA, April 27-30, 1998.

<sup>3</sup>Whitmore, S.A., and Dunbar, B.J., "Orbital Space Plane: Past, Present, and Future," AIAA-2003-2718, AIAA/ICAS International Air and Space Symposium and Exposition: The Next 100 Years", Dayton, Ohio, 14-17 July 2003.

<sup>4</sup>Janicik, J.L., "The Phase I Space Maneuver Vehicle Test Program - Leading the United States into the 21st Century," AIAA-1999-4539, AIAA Space Technology Conference and Exposition, Albuquerque, New Mexico, Sept. 28-30, 1999.

<sup>5</sup>Rausch, V., and McClinton, C., "NASA's Hyper-X Program," IAF-00-V.4.01, 51st International Astronautical Congress, Rio de Janeiro, Brazil, 2-6 October 2000.

<sup>6</sup>Bradford, J. E., Charania, A., Wallace, J. and Eklund, D. R., "*Quicksat*: A Two-Stage to Orbit Reusable Launch Vehicle Utilizing Air-Breathing Propulsion for Responsive Space Access," AIAA-2004-5950, Space 2004 Conference and Exhibit, San Diego, California, September 28-30, 2004.

<sup>7</sup>Phoenix Integration, Inc., web site, on-line, Internet, 31 August 2004, available from: <http://www.phoenix-int.com>.

<sup>8</sup>Brauer, G. L., D. E. Cornick, and Stevenson, R., "Capabilities and Applications of the Program to Optimize Simulated Trajectories," NASA CR 2770. February, 1977.

<sup>9</sup>Sova, G., and Divan, P., "Aerodynamic Preliminary Analysis System II, Part II D User's Manual," NASA CR 182077, April, 1991.

<sup>10</sup>Numerical Aerodynamic Simulation via CARTesian Grid Techniques, Department of Aerospace Engineering, Georgia Institute of Technology, Atlanta, Georgia, on-line, Internet, 31 August 2004, available from: <http://www.ae.gatech.edu/~sruffin/nascart>.

<sup>11</sup>Klann, J. L.; Snyder, C. A.: NEPP Programmers Manual (NASA Engine Performance Program) Volume 1. Technical Description: NASA Technical Memorandum 106575, September 1994, on-line, Internet, 31 August 2004, available from: [http://www-psao.grc.nasa.gov/asaonepp\\_code\\_pub.html](http://www-psao.grc.nasa.gov/asaonepp_code_pub.html).

<sup>12</sup>Rocket Engine Design Tool for Optimal Performance (REDTOP), <http://sei.aero/products/redtopoverview.html>

<sup>13</sup>Bradford, J. E., Charania, A., St. Germain, B., "REDTOP-2: Rocket Engine Design Tool Featuring Engine Performance, Weight, Cost, and Reliability," AIAA-2004-3514, 40th AIAA ASME/SAE/ASEE Joint Propulsion Conference and Exhibit, Fort Lauderdale, Florida, July 11-14, 2004.

<sup>14</sup>Colket, M. B. III and Spadaccini, L. J., "Scramjet Fuels Autoignition Study," *Journal of Propulsion and Power*, Vol. 17, No.2, March-April 2001, pp. 315-323.

<sup>15</sup>Cadman, P, Thomas, G. O. and Butler, P., "The auto-ignition of propane at intermediate temperatures and high pressures," *Phys. Chem. Chem. Phys.*, Vol. 2, 2002, pp. 5411-5419.